Real-time optical CD metrology for litho proces

J. L. Opsal, Y. Wen, J. Lee, W. L. Smith
Therma-Wave, Inc., 1250 Reliance Way, Fremont, CA 94539

ABSTRACT

In this work we present results of 193 nm stepper studies involving several thousand sites per wafer to examine the CD behavior over the FEM, and compare with traditional results from top-down CD-SEM and cross-section SEM. This study establishes that optical CD metrology offers new and useful characteristics to optimize advanced litho processes and indeed is developing into a viable alternative to the CD-SEM.

Keywords : Real-time, CD, metrology, scatterometry lithography

1. INTRODUCTION

Real-time optical CD metrology[1], employing fast numerical solutions to the diffraction of light from microelectronic features, is beginning to gain wide usage for sub-130nm IC processing. Applications of this method heretofore have concentrated on two steps in the patterning process: the "develop inspect" (DI) step, at which point the pattern features are formed in the photoresist but prior to etch, and the "final inspect" (FI) step, after the etch process has transferred the feature into the underlying IC layer(s). In this article, we examine another application: use of optical CD metrology for rapid characterization of stepper/scanner performance and optimization.

In order to be useful to characterize a litho process, we found it necessary to expand the set of fitting parameters to include the pitch of the measured line/space array ("grating"). This is due to two practical matters: first, the pitch imprinted on a wafer is the result of the pitch on reticle and second, the pitch on the wafer is a result of imaging magnification. As a result, this parameter can vary by several percent typically, for a pitch target of 240 to 350 nm. Without taking this parameter into account, high-quality fitting of results over a full-field focus-exposure matrix (FEM) wafer, for example, is problematic. With the pitch included as a fitting parameter, it is possible to obtain excellent data-model fits across an entire FEM with a single metrology recipe.

2. SAMPLE AND MEASUREMENTS

A series of line/space (L/S) features were exposed and developed on a film stack of 193 nm photo resist (2000 ~ 3000 Å) over an organic Barc layer (~ 820 Å) on a 200 mm crystalline Silicon substrate. The substrates were processed under recommended conditions provided by ASML (4800 Great America Parkway, Santa Clara, CA 95054).

Measurements were taken on an Opti-Probe 5340 system equipped with rotating compensator spectral ellipsometer (RCSE)[1] of Therma-Wave (1250 Reliance Way, Fremont, CA 94539). Data were analyzed using RT/CD technology[2] of Therma-Wave as illustrated in Figure 1 to determine cross-section profiles as well as thickness of Barc layer, and pitch. The Weir Analysis[3] of TEA system Corp. (65 Schlossburg St., Alburtis, PA 18011) was used for analyzing litho process variation.

3. RESULTS AND DISCUSSION

3.1 Exposure meander
An analysis of exposure sensitivity was performed by creating an exposure matrix (EM) of 57 fields. Exposure energy varied from 25 mJ to 11.5 mJ with 0.25 mJ per step. The analysis measured eleven (11) sites per field on each exposure.

Figure 2 shows RT/CD results of CDs at 50% (Middle), and 20% (Bottom) of line height, photoresist thickness (line height), and the corresponding goodness of fit (GOF).

All measurements were taken using a single RTCD recipe. Those fields exhibiting a relatively low GOF, as blocked within the rectangular box, were the result of poorly defined L/S structures.

Results here show a clear, linear relationship between CDs and exposure energy down to 15 mJ with high sensitivity. The CD profile map for this EM0 is illustrated in Figure 3. The corresponding measured and model spectra of site 1 of Figure 3 are presented in Figure 4.

3.2 Focus sensitivity
Exposure energy and focus errors are the two key parameters of the lithography process. Any metrology recipe must be able to cope with variations in both for a range covering the normal excursions of the process.

Figure 5 presents the RTCD results of a focus meander with a range between –0.9 µm and 0.9 µm in 0.025 µm steps. The metrology recipe for this exhibits a valid response over a focus variation range of ± 0.2 µm. This range represents a functional scope that exceeds the typical focus variation found in production at this design level.

The corresponding CD profile map for the entire +/-0.9 µm range is shown in Figure 6.

3.3 Pitch variation induced by CD bias
Isolated and dense packed device features respond differently to actinic radiation during the exposure process. Consequently, they will also exhibit quite different characteristics when measured using scatter or ellipsometric techniques. The ability of a metrology tool to accurately measured both of these structures is therefore critical for robust production performance.

In order to prove the flexibility of RTCD technology, two sets of dense and isolate L/S structures were prepared with variations of pitch induced by CD bias in the design. RTCD recipes with floating pitch values have been developed for both dense and isolate structures.

Figure 7 shows the RTCD measured response across the CD bias range for three sets of pitch values in both dense (left image) and isolated (right image) line-space pairs. Notice the anticipated linear response of the measured pitch across both sets of values.

Isolated line performance will be more sensitive to substrate and BARC uniformity as well as reticle design address-aliasing. This sensitivity can be seen in the fine structure of the three curves on the right side of the figure.

3.4 Focus-exposure matrix (FEM)
A focus-exposure matrix is a common process design tool for the optimal centering of focus and exposure. In this study, a developed FEM wafer was analyzed using the RTCD technology. Figure 8 illustrates two 3-D contour plots of middle CDs and photo resist thickness which provides a typical bowl pattern or Bossung plot. These plots, when used in conjunction with the RTCD detail profiles at each field, establish the techniques as an efficient tool for process window calculation.

3.5 Analysis of litho process variation

3.5.1 Macro/micro uniformity
Up to this point, this analysis has solely addressed the ability of RTCD to determine feature variations resulting from deviations in focus and exposure. However device dimensional perturbations are influenced by more than these two exposure factors and the static signature of feature variations resident on the reticle. Dimensions are influenced by factors such as underlying films, photoresist thickness and localized variations in exposure and leveling. Final feature sizes will respond to all these perturbations plus the variation in Side-wall-angle (SWA) or the slope of the cross-sectional photoresist profile. RTCD technology provides critical in-site into all these factors.

The contour plots of Figure 8 address the RTCD measured variation of BCD (CD at 20% of line height), photoresist thickness, Barc thickness, and sidewall angle within each field and across the substrate.

The as-measured BCD variation across the substrate can be seen in Figure 9(a). This contour of CD uniformity exhibits the contributions of wafer non-uniformity and across-field variation after develop.

Non-uniformity across the substrate can contribute significantly to the perturbation spectrum. Applying a model to wafer-based parameters allows the analysis to remove these from observation. Figure 9(b) shows the variation in side-wall-angle of the photoresist profile after the influences of wafer systematic tilt and bow have been removed.

Photoresist film uniformity is critical when considering the effects of deposition, wafer tilt, wafer bow and spray-puddle developing. To view the influence of these factors on photoresist, the average field was removed from the data and plotted as a wafer contour in Figure 9(c). Notice both the puddle effects on the left side of the substrate and the spiraled spin striations after removal of corresponding field mean.

BARC uniformity is critical for uniform standing wave and resist-profile foot reproduction. In Figure 9(d) the field average BARC variation and the wafer aberrations have been removed to display the deposition uniformity of the antireflective undercoating. A film height profile plot is shown in the XY plot immediately to the left of the figure. Notice the low-level minimum in the wafer center and associated radii.

Combining RTCD with a sophisticated analysis tool as Weir Analysis used here can provide an efficient solution to characterize and monitor litho process variation in production line.

3.5.2 Focus behavior within field and across wafer
One wafer was processed with four fields exhibiting focus errors ranging from the best focus to + 0.4 µm defocus. This four-field pattern was repeated on a second row. The focus layout is shown in Figure 10(a) and the perturbed exposures as two sets of circled fields in Figure 10(b).

A contour plot of MCD (CD at 50% line height) variation across the global of that wafer excluding outliners is presented in Figure 10(b). Figure 10(b) plots the MCD variation after wafer systematic errors have been removed.

Figure 10(b) clearly shows significant pattern difference at those skewed fields. Figures 11 and 12 show MCD variation vs. each field, and the same selected site in each field in the same row. The results show clearly on i) sensitivity for a broad focus range as pointed out early, ii) the Bossung pattern of CD vs. focus offset.

3.5.3 Field Magnification errors
Field magnification was varied on two fields by +/- 2 ppm by slightly tilting the reticle at two selected fields as shown in Figure 13. The XY plot derived from the two adjacent fields exhibit the anticipated mirror image distribution as illustrated in solid line. Similarly to CDs, there is difference in pitch distribution pattern associated with magnification changes.

3.5.4 Reticle tilt effect
Image tilt from both the wafer stage and reticle contribute to process variations in feature uniformity. Figure 14 shows BCD change within selected fields associated with tilt of reticle along X-axis at sub µrad scale. The tilting angles were determined based on BCD variation within a specific field. The modeled variations are shown in the table at the bottom of the figure.

4. CONCLUSIONS

With the information-rich information content of the RCSE we have demonstrated very good sensitivity and robustness of the RTCD technology to small changes over wide ranges of pitch, focus and exposure on lithographically significant resist structures.

REFERENCES

1. J. Opsal, J. Fanton, J. Chen, J. Leng, L. Wei, C. Uhrich, M. Senko, C. Zaiser, and D. E. Aspnes, "Broadband spectral operation of a rotating-compensator ellipsometer", Thin Solid Films 313-314, 58-61 (1998).
2. J. Opsal, H. Chu, Y. Wen, Y.C. Chang and G. Li, "Fundamental solutions for real-time optical CD metrology", Metrology, Inspection, and Process Control for Lithography XVI, Daniel J. C. Herr, Editor, Proceedings of SPIE Vol. 4689,163-176 (2002).
3. T. Zavecz, S. Hsu, "Controlling Focal Plane Tilt", Semiconductor International, March 1999.
4. M. Dusa, B. Su, S. Dellarochetta, T. Zavecz, "Photo-lithographic lens characterization of critical dimension variation using empirical focal plane modeling", SPIE Vol 3051-26 (1997)
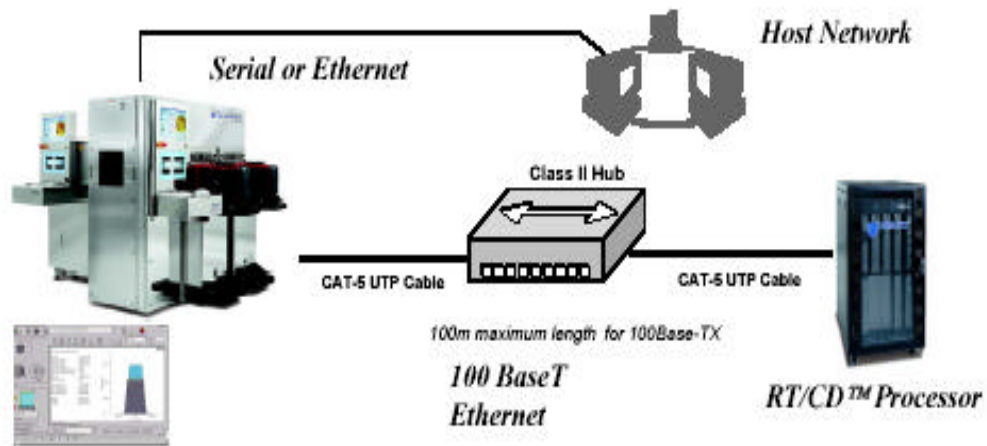
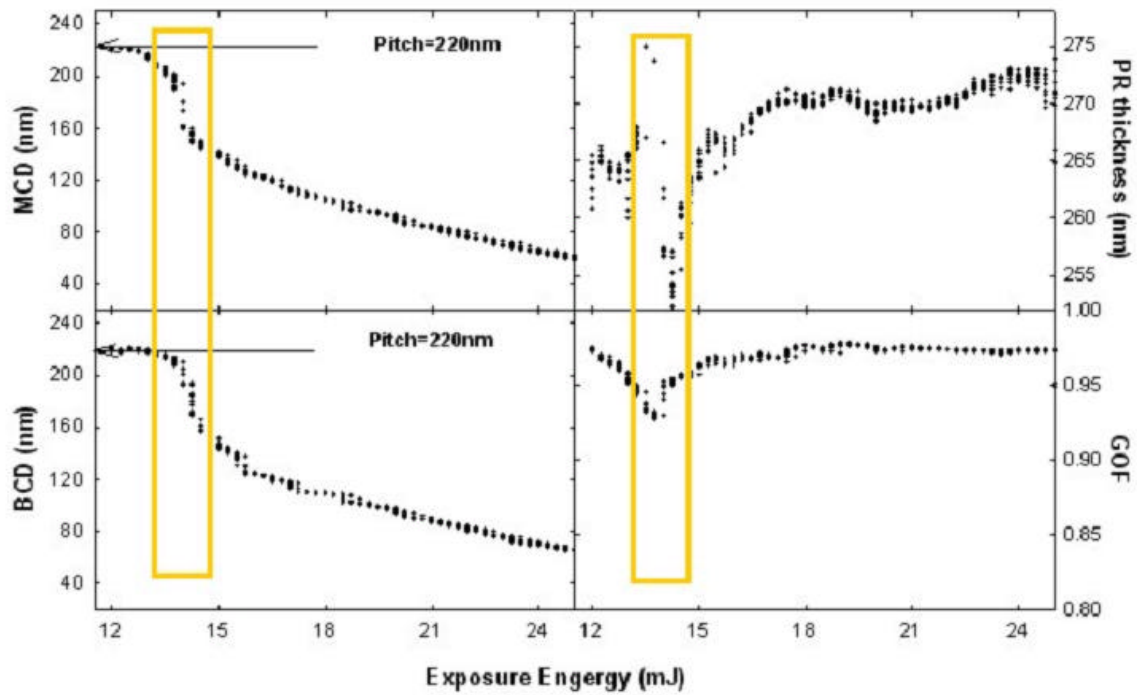Figure 1: Diagram of RT/CD^{TM} technology.

Figure 2: CD linearity from 60 nm to 120 nm as a function of exposure energy at 0.25 mJ/step.
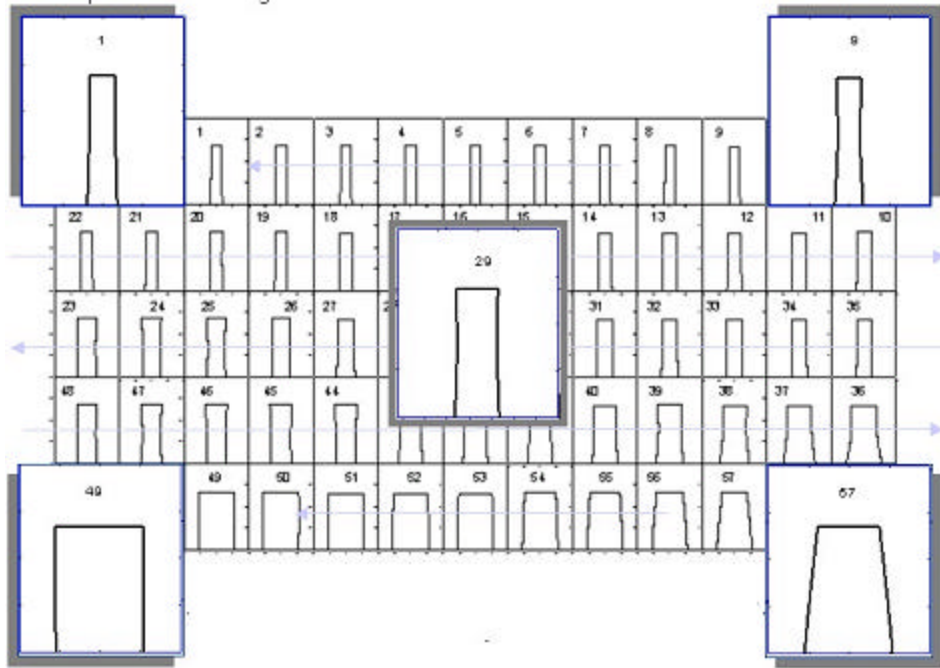
Figure 3: Profile map of all 57 fields for the EM. the pop -out plots are enlarged metrology profiles at five selected fields. The arrows show the exposure scan direction.
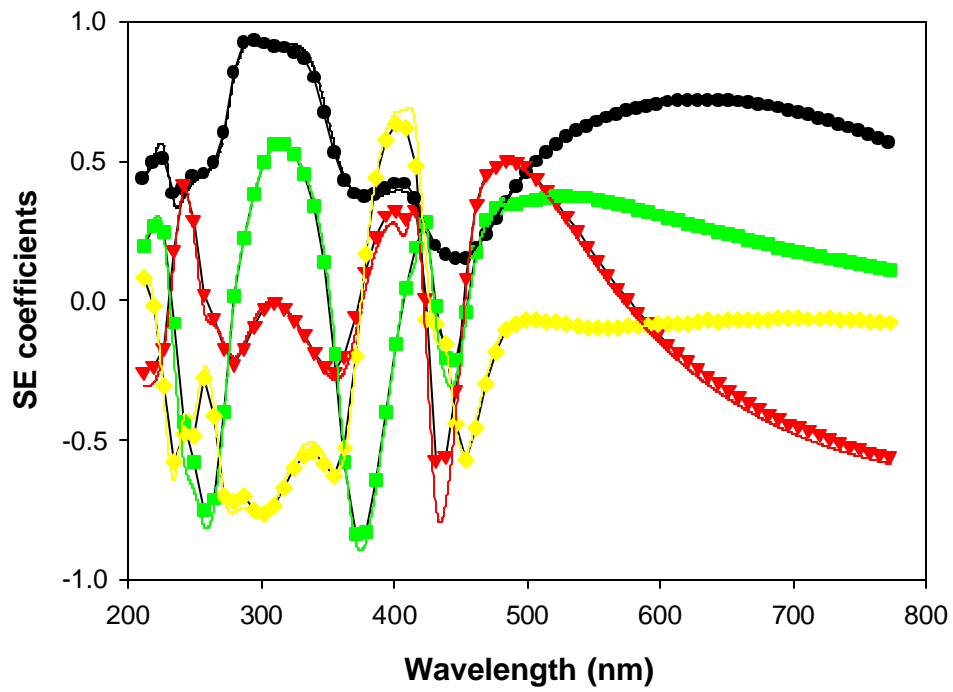
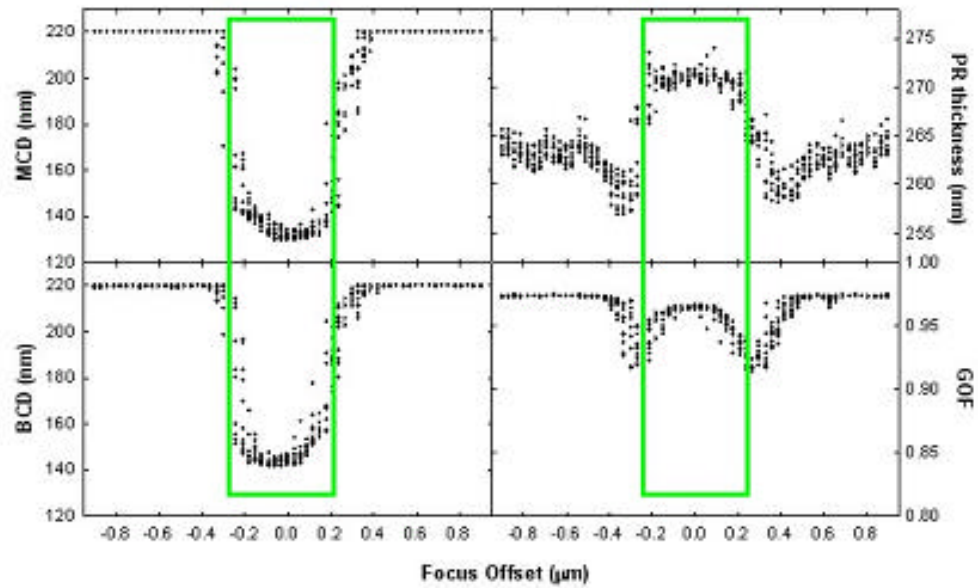Figure 4.: Measured (symbols) and model (solid lines) spectra of site 1 of Figure 2.

Figure 5: Sensitivity of the RTCD model across a broad focus range of +/- 0.2 mm at 0.025mm/step.
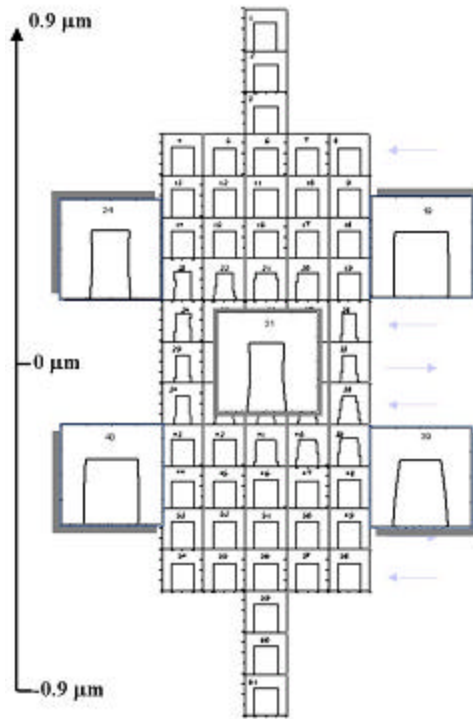
Figure 6: Profile map of all 61 fields under the FM meander, the pop -out plots are enlarged profile at five selected fields. The arrows show the focus scan direction.
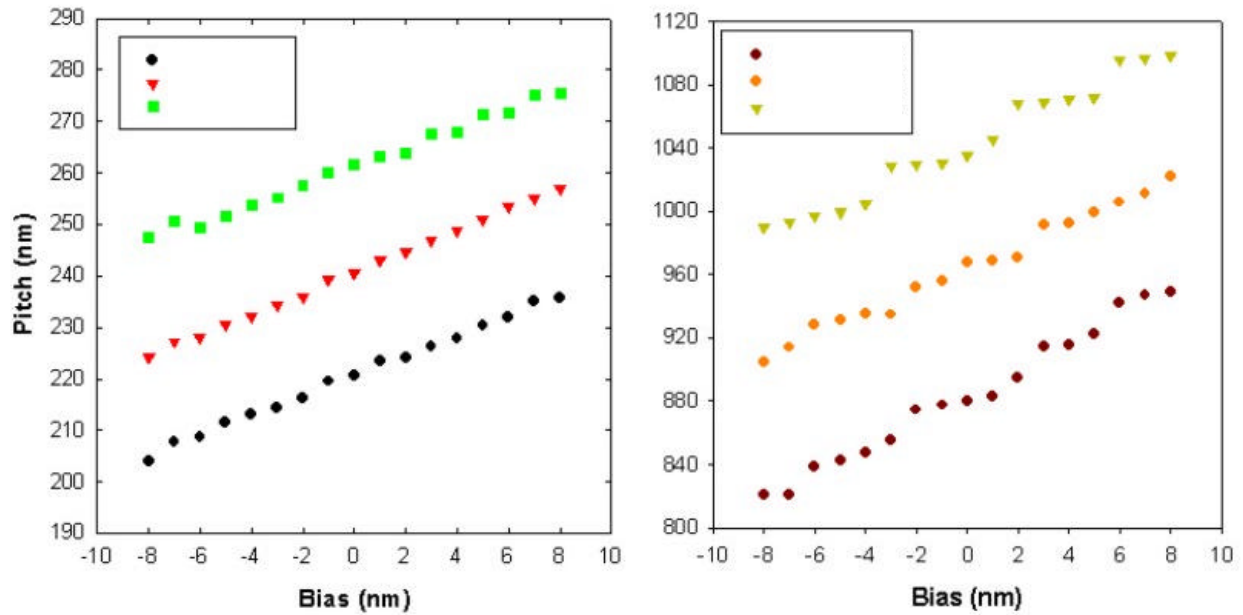

Figure 7: Pitch varies from 210 nm to 280 nm (left plots), and from 820 nm to 1100 nm (right plots) over a CD bias range {-8 nm, 8 nm}.
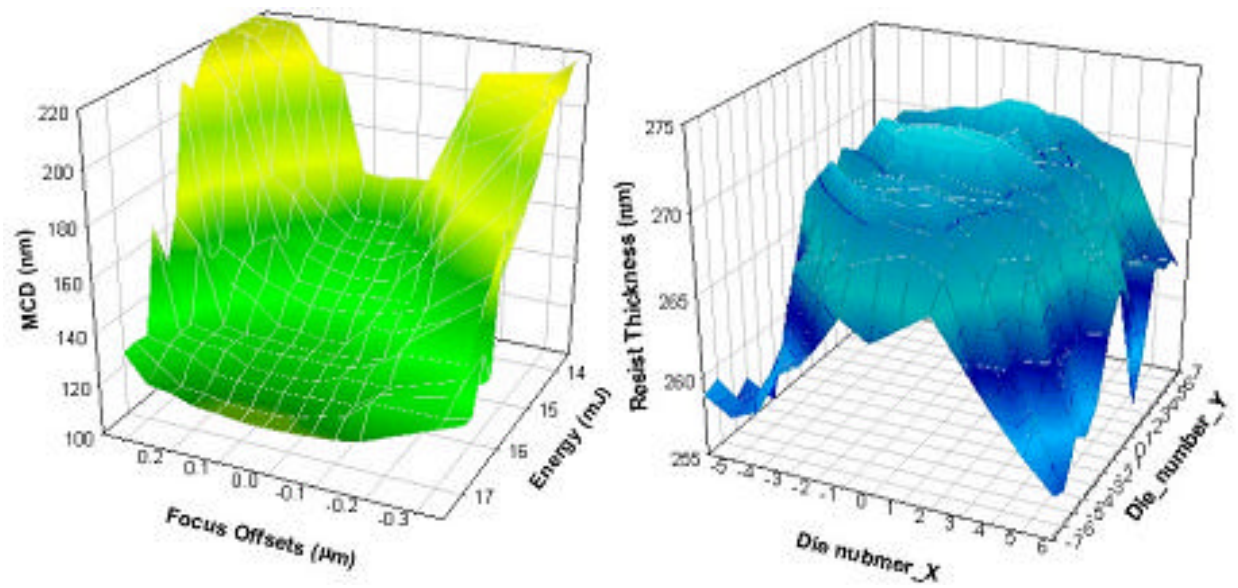
Figure 8: Provide thickness and CD results across entire FEM range with features from approximately 100 nm up to full pitch of 220 nm.

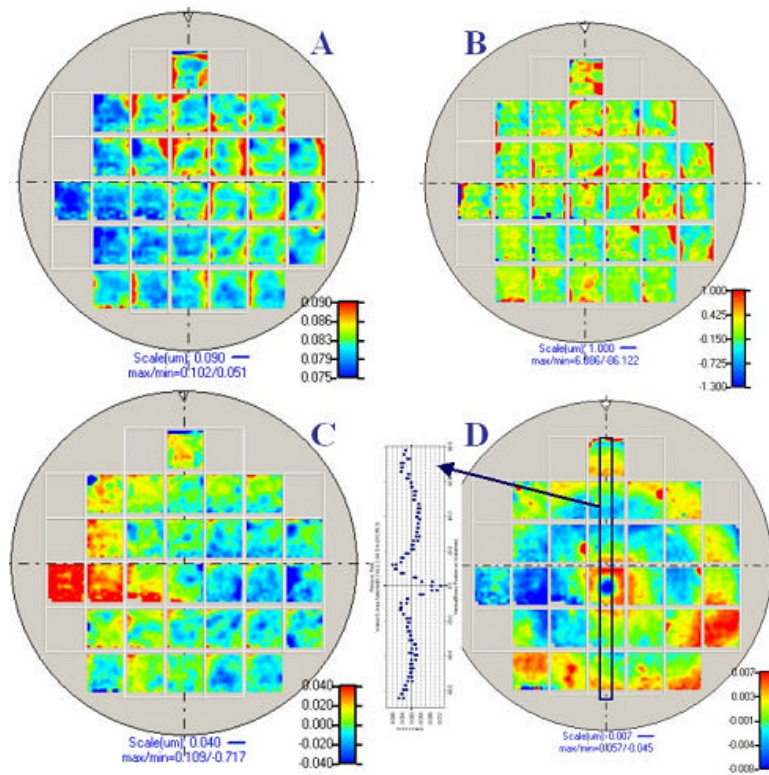Figure 9: Field/wafer variation of (a) BCD, (b) sidewall angle, (c) resist, and (d) Barc thickness.
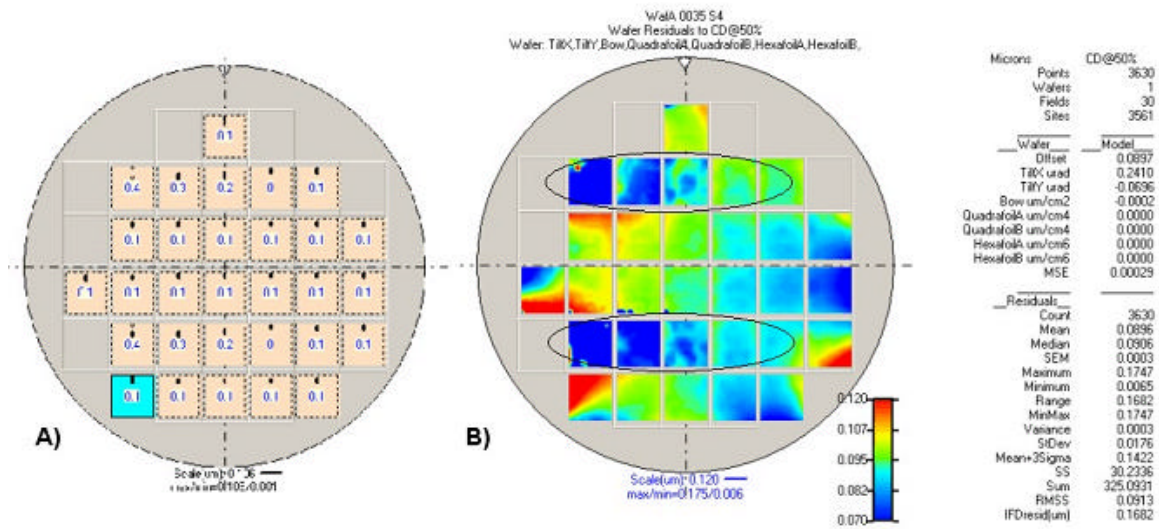
Figure 10: (a) Wafer layout with different focus offset per field, and (b) Raw MCD contour plots at all fields.
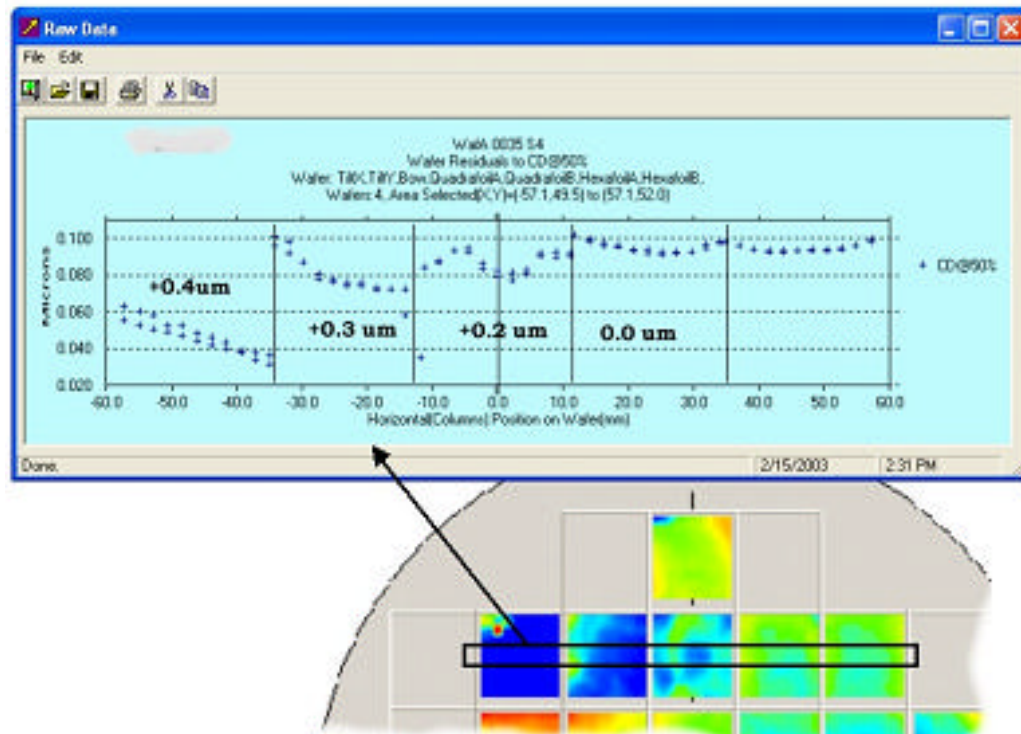

Figure 11: Raw MCDs in five selected fields with different focus offsets at 0.1 mm focus increments per field.
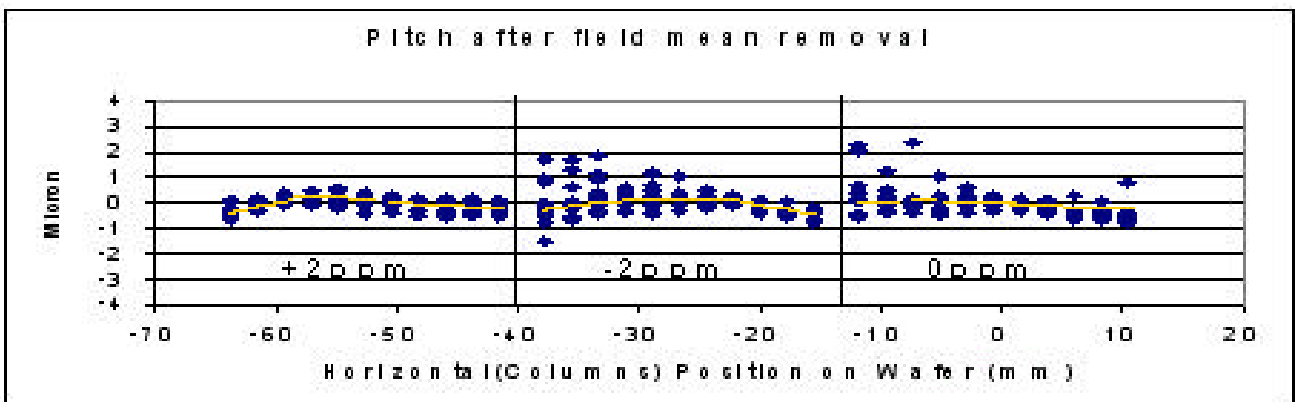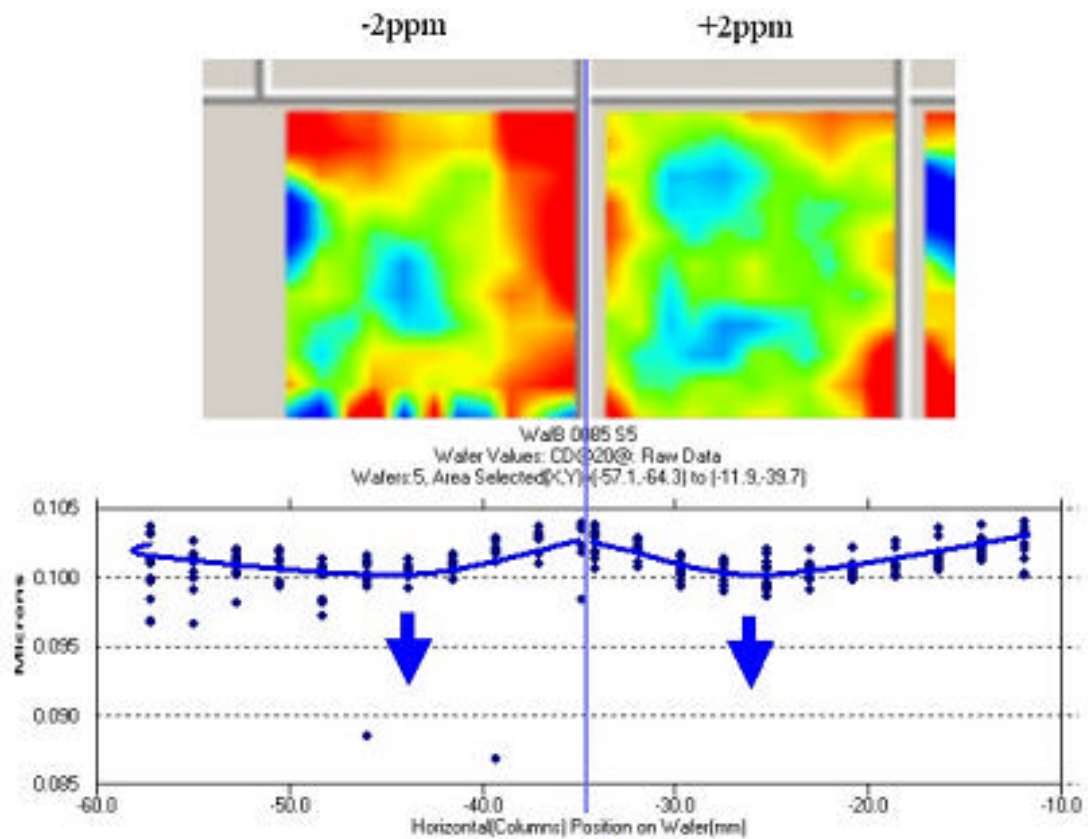
Figure 13: BCD and pitch distribution changes due to variation of field magnification errors.

WafD 0037 S7
Wafer Values: CD@20@
Wafer: None /Field: All Coefs

Microns	CD@20@
Points	484
Wafers	1
Fields	4
Sites	484

Wafer	Model
Offset	0.0838
TiltX urad	0.0954
TiltY urad	-0.0193
Bow um/cm2	0.0000
QuadrafoilA um/cm4	0.0000
QuadrafoilB um/cm4	0.0000
HexafoilA um/cm6	0.0000
HexafoilB um/cm6	0.0000
MSE	0.00001

Field	Model
Piston	0.0811
TiltX urad	-0.1652
TiltY urad	-0.0487
CurvX um/cm2	0.0036
CurvY um/cm2	0.0015
MSE	0.00001

Fitted	
Count	484
Mean	0.0838
Median	0.0857

3
10
30 29

Scale(um) 0.092 —
max/min=0.092/0.080

0.092
0.089
0.086
0.083
0.080

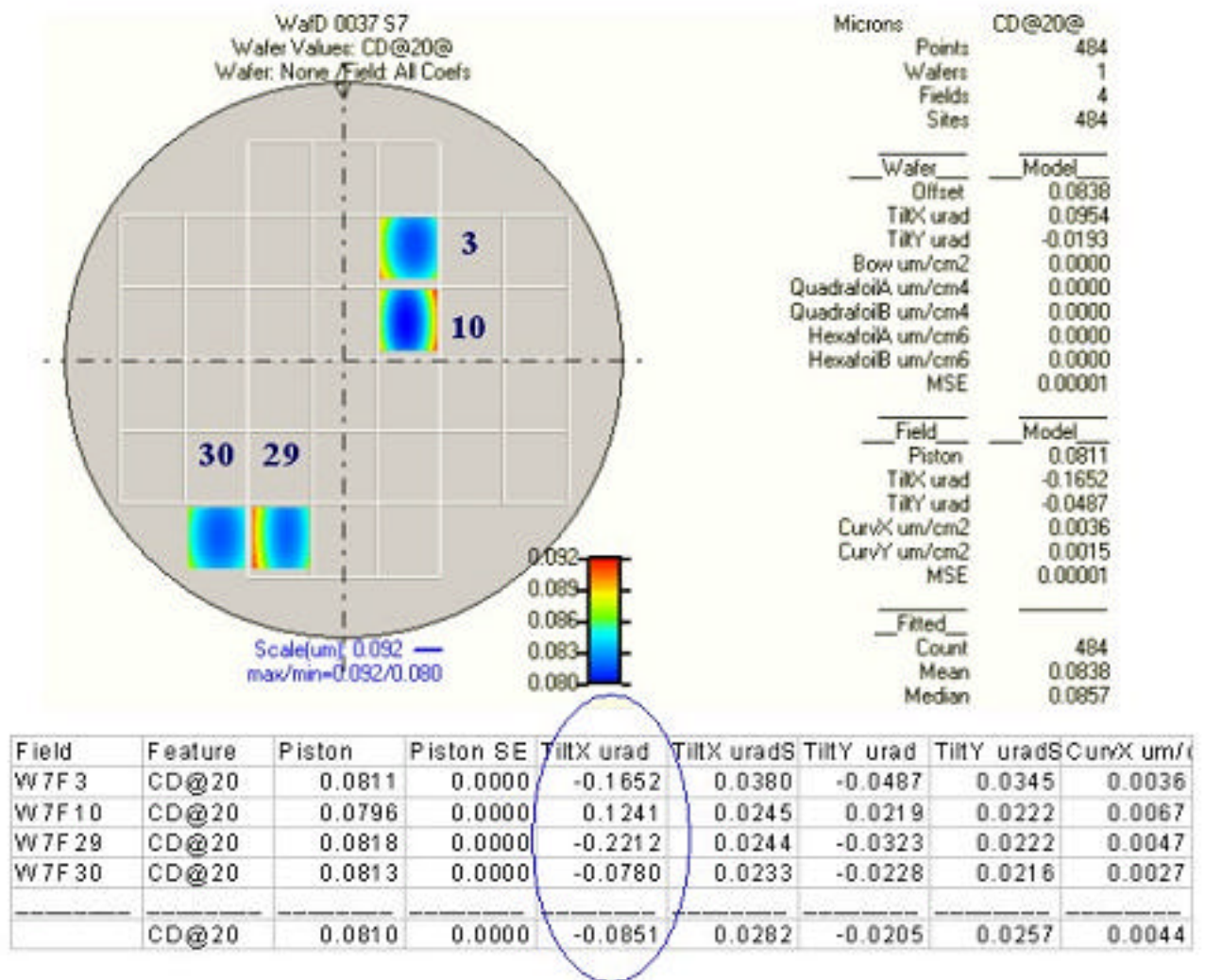| Field	Feature	Piston	Piston SE	TiltX urad	TiltX uradS	TiltY urad	TiltY uradS	CurvX um/c
W7F3	CD@20	0.0811	0.0000	-0.1652	0.0380	-0.0487	0.0345	0.0036
W7F10	CD@20	0.0796	0.0000	0.1241	0.0245	0.0219	0.0222	0.0067
W7F29	CD@20	0.0818	0.0000	-0.2212	0.0244	-0.0323	0.0222	0.0047
W7F30	CD@20	0.0813	0.0000	-0.0780	0.0233	-0.0228	0.0216	0.0027
	CD@20	0.0810	0.0000	-0.0851	0.0282	-0.0205	0.0257	0.0044

Figure 14: BCD variation after removal of mean of the field and systematic at selected fields due to reticle tilting.